Electronic Supplementary Material (ESI)

Low cost triazatruxene hole transporting material for >20% efficient perovskite solar cells

Arthur Connell[a], Zhiping Wang[b*] Yen-Hung Lin[b], Peter C. Greenwood[a], Alan A. Wiles[c], Eurig W. Jones[a], Leo Furnell[a], Rosie Anthony[a], Christopher P. Kershaw[a], Graeme Cooke[c], Henry. J. Snaith[b*] and Peter J. Holliman[a*]

[a] College of Engineering, Bay Campus, Swansea University, Swansea, SA1 8EN, UK.
[b] Dept of Physics, University of Oxford, Clarendon Laboratory, Parks Road, Oxford OX1 3PU, UK.
[c] Glasgow Centre for Physical Organic Chemistry (GCPOC), WestCHEM, School of Chemistry, University of Glasgow, Glasgow, G12 8QQ, UK.

S1 – Synthesis

10,15-dihydro-5H-diindolo[3,2-a:3',2'-c]carbazole (2).
A mixture of oxindole (10 g, 75 mmol) and $POCl_3$ (50 mL) was heated at 100 °C for 6h. The cooled reaction mixture was slowly poured into crushed ice water so that a temperature of less than 10 °C was maintained. This mixture was neutralized carefully with a saturated KOH solution added in small quantities so that a temperature of less than 10 °C was maintained. After neutralization, the precipitate was filtered to give the crude product as a brown solid. The crude solution in MeOH was absorbed on silica-gel, dried, loaded and eluted through a thick silica-gel pad with a CH_2Cl_2 as a mobile phase. After evaporation of the solvent at reduced pressure and recrystallization from acetone, a white solid was obtained. (5.5 g, 65 %). ^{1}H NMR (400 MHz, DMSO-d6) δ 11.86 (s, 3H), 8.68 (d, J = 7.6 Hz, 3H), 7.73 (d, J = 7.8 Hz, 3H), 7.41 – 7.32 (m, 6H). ^{13}C NMR (100 MHz, DMSO-d6) δ 141.0, 135.3, 123.6, 124.1, 120.9, 120.4, 111.8, 103.1. $C_{24}H_{15}N_3$[M+H$^+$] Exact Mass = 346.1341, MS (FTMS + p NSI) = 346.1341.

5,10,15-trihexyl-10,15-dihydro-5H-diindolo[3,2-a:3',2'-c]carbazole (3). To a solution of **(1)** (1 g, 2.90 mmol, 1 eq.) in DMF (20 mL), NaH (0.2 g, 10.2 mmol, 3.5 eq.) was added at room temperature and stirred for half hour. Then 1-iodohexane (2.46 g, 11.6 mmol, 4 eq.) was added *via* a syringe and the mixture was heated at 160 °C i.e. refluxed for 2h. The cooled mixture was poured into water and extracted with CH_2Cl_2. The organic phase was dried over $MgSO_4$. The product was isolated off on a silica gel column with 20 % CH_2Cl_2 in petroleum ether to give **(3)** as a pale yellow solid (1.3 g, 75%). ^{1}H NMR (400 MHz, Chloroform-d) δ 8.21 (d, J = 8.0 Hz, 3H), 7.55 (d, J = 8.1 Hz, 3H), 7.37 (t, J = 7.6 Hz, 3H), 7.25 (t, J = 7.5 Hz, 3H), 4.92-4.76 (m, 6H), 1.90 (dt, J = 15.4, 7.8 Hz, 6H), 1.23 – 1.11 (m, 18H), 0.79 (t, J = 6.9 Hz, 9H). ^{13}C NMR (100 MHz, Chloroform-d) δ 13.83, 20.44, 24.70, 29.05, 31.06, 43.70, 106.14, 109.32, 119.60, 118.84, 120.55, 126.60, 138.14, 139.19. $C_{42}H_{51}N_3$[M+H$^+$] Exact Mass = 598.4158, MS (FTMS + p NSI) = 598.4158.

3,8,13-tribromo-5,10,15-trihexyl-10,15-dihydro-5H-diindolo[3,2-a:3',2'-c]carbazole (4).
To a solution of **(3)** (1 g, 1.66 mmol, 1 eq.) in 90 mL $CHCl_3$, (915 mg, 5.15 mmol, 3.1 eq.) of NBS in 15 mL DMF was added dropwise *via* a syringe at 0 ºC. After addition, the reaction mixture was stirred for 1h at room temperature. The mixture was extracted with CH_2Cl_2 and the organic phase was dried over $MgSO_4$. The product was isolated on a silica gel column with 10 % CH_2Cl_2 in petroleum-ether to give a product as a white solid (1.35 g, 82%). ^{1}H NMR (400 MHz, Chloroform-d) δ 8.03 (s, 3H), 7.71 (s, 3H), 7.33 (d, J = 7.1 Hz, 3H), 4.65 – 4.59 (m, 6H), 1.83 – 1.62 (m, 6H), 1.35 – 1.14 (m, 18H), 0.72 (m, 9H). ^{13}C NMR (400 MHz, Chloroform-d) δ 127.3, 123.4, 122.2,

123.0, 121.1, 120.6, 112.1, 111.0, 52.6, 45.3, 30.7, 28.3, 25.7, 21.6, 12.1. $C_{42}H_{48}Br_3N_3$[M+H] Exact Mass = 832.1486, MS (+ive ESI-QTOF) = 832.1486.

S1a NMR spectrum of (2)

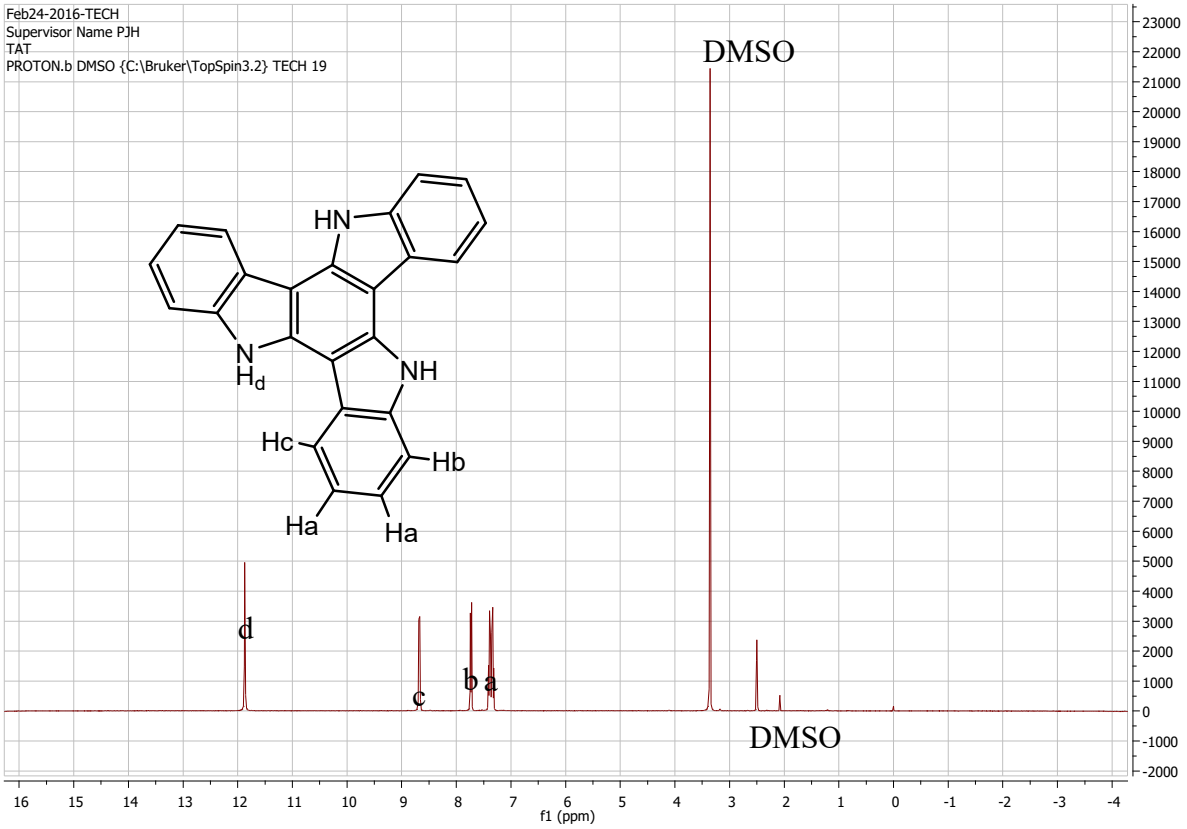

S1b NMR spectrum of (3)

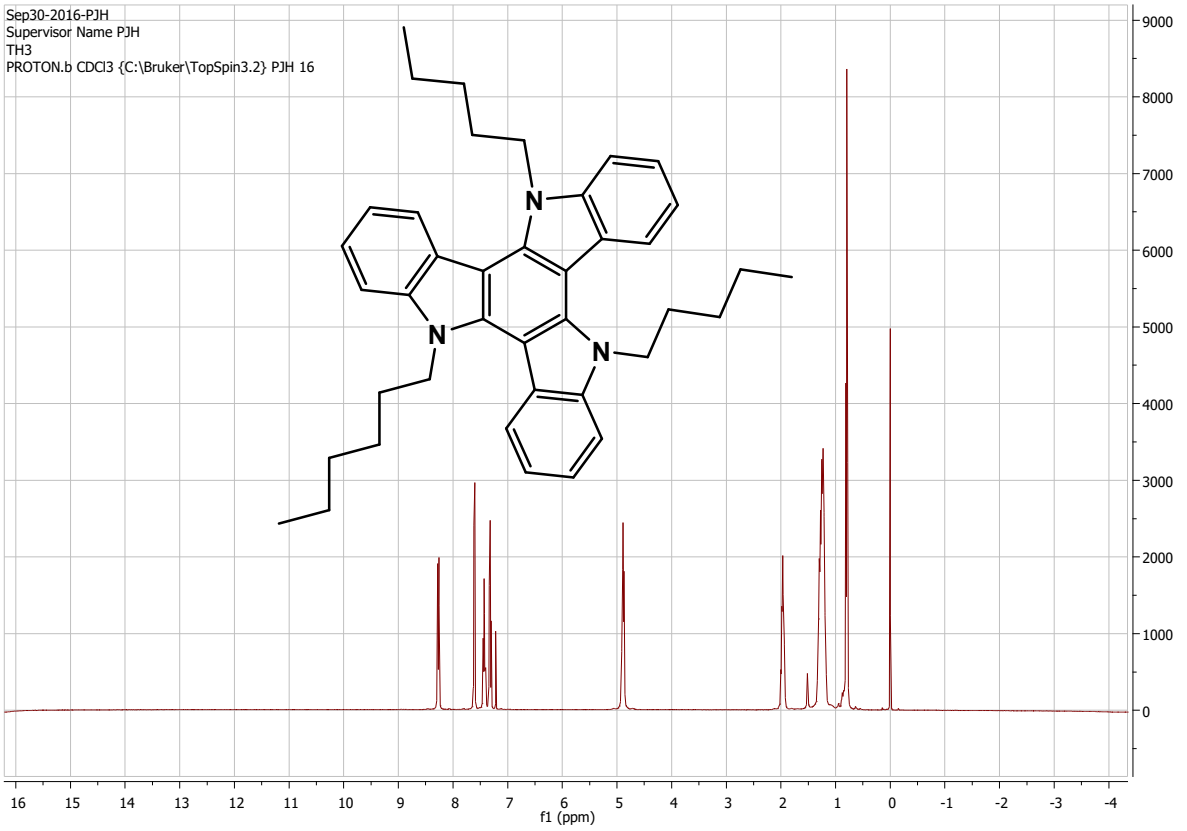

S1c NMR spectrum of (4)

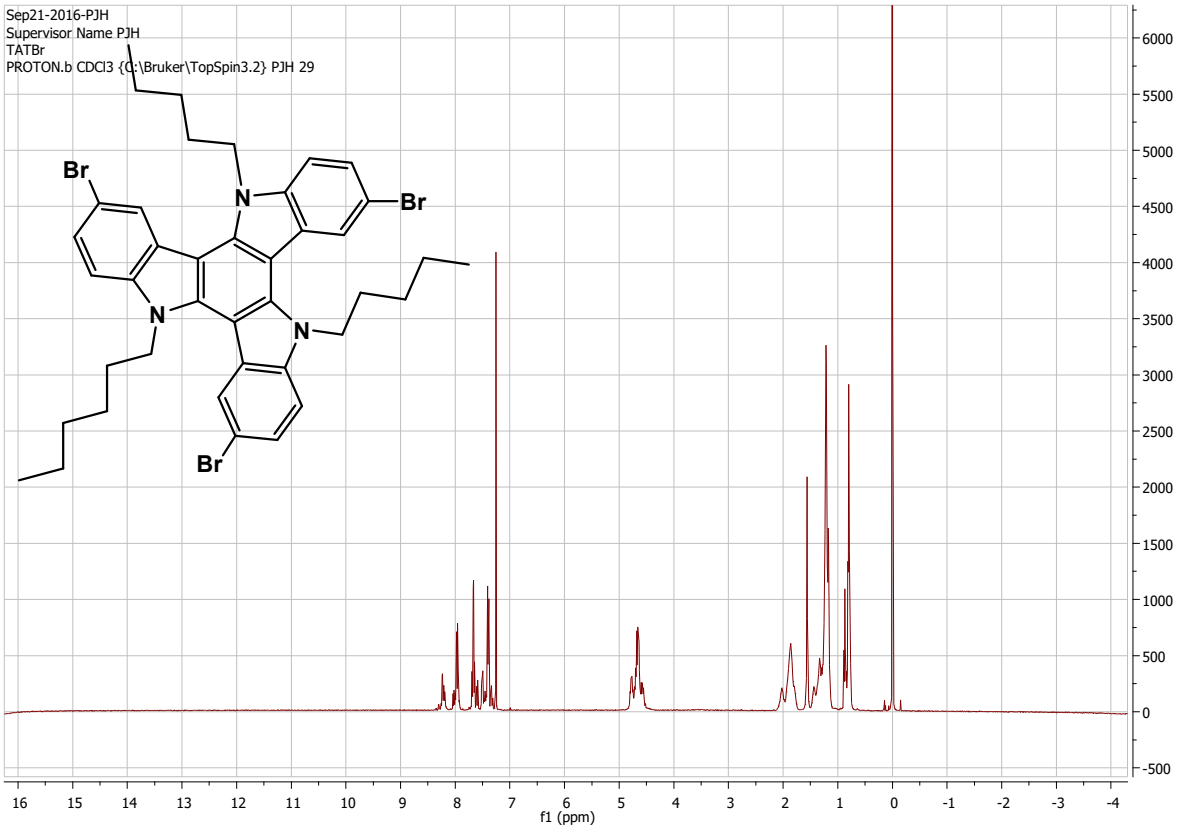

S2 Full ^{1}H NMR Spectrum for TAT-^{t}BuSty with peak picking and integration analysis

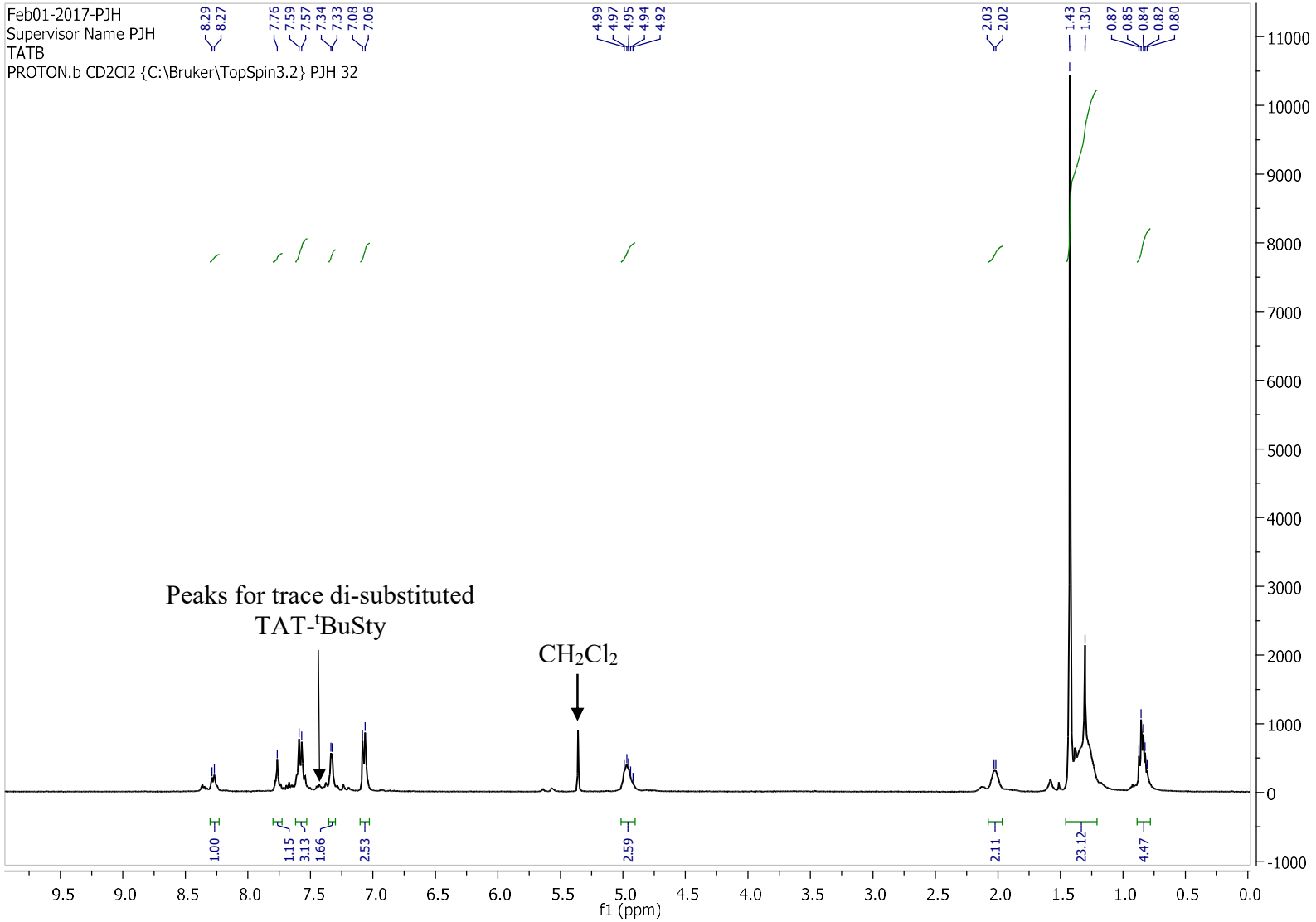

S2.1 Theoretical estimation of ^{1}H NMR peaks

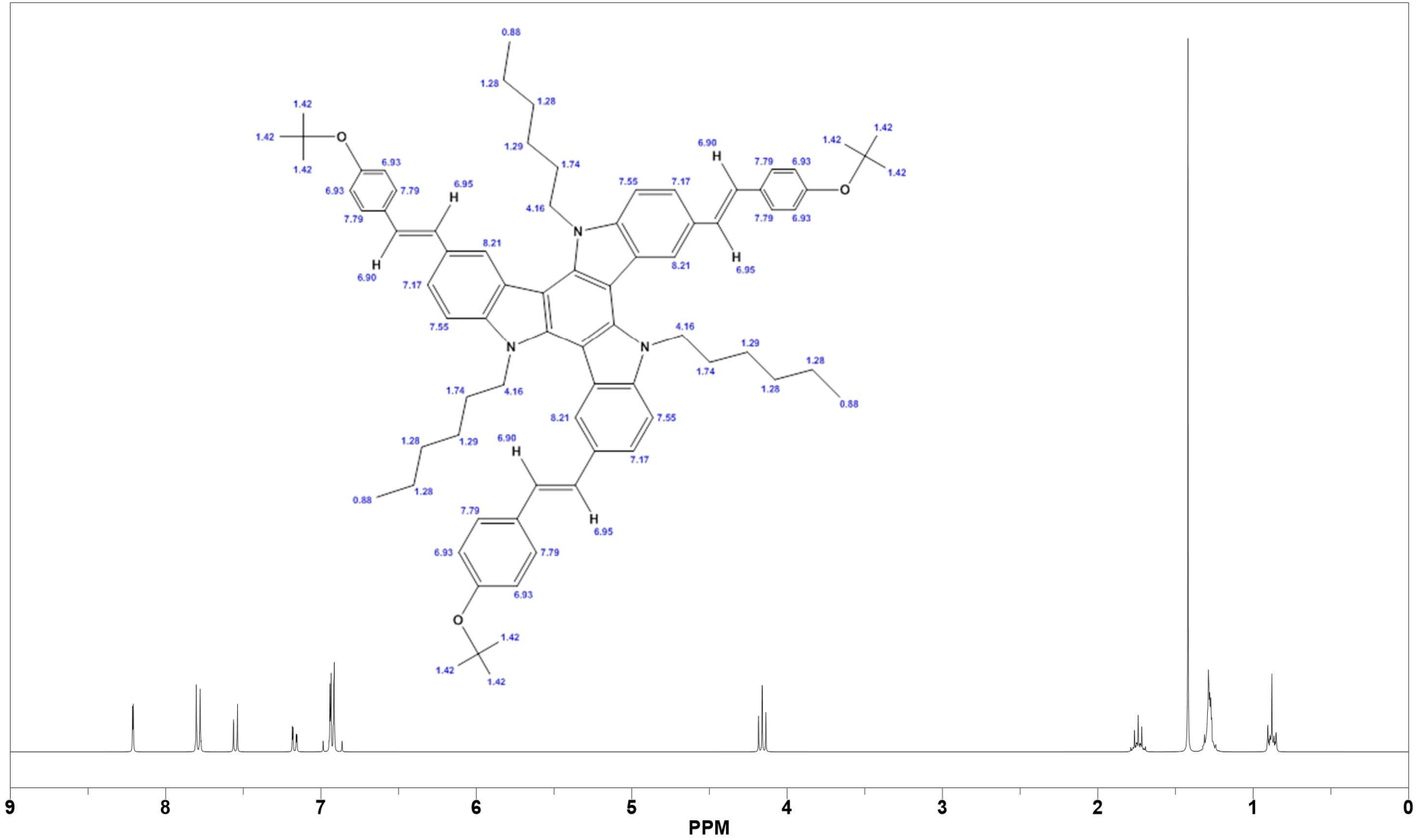

S2.2 Expansion of aromatic resonance region of ^{1}H NMR spectrum of TAT-^{t}BuSty with peak picking and integration analysis

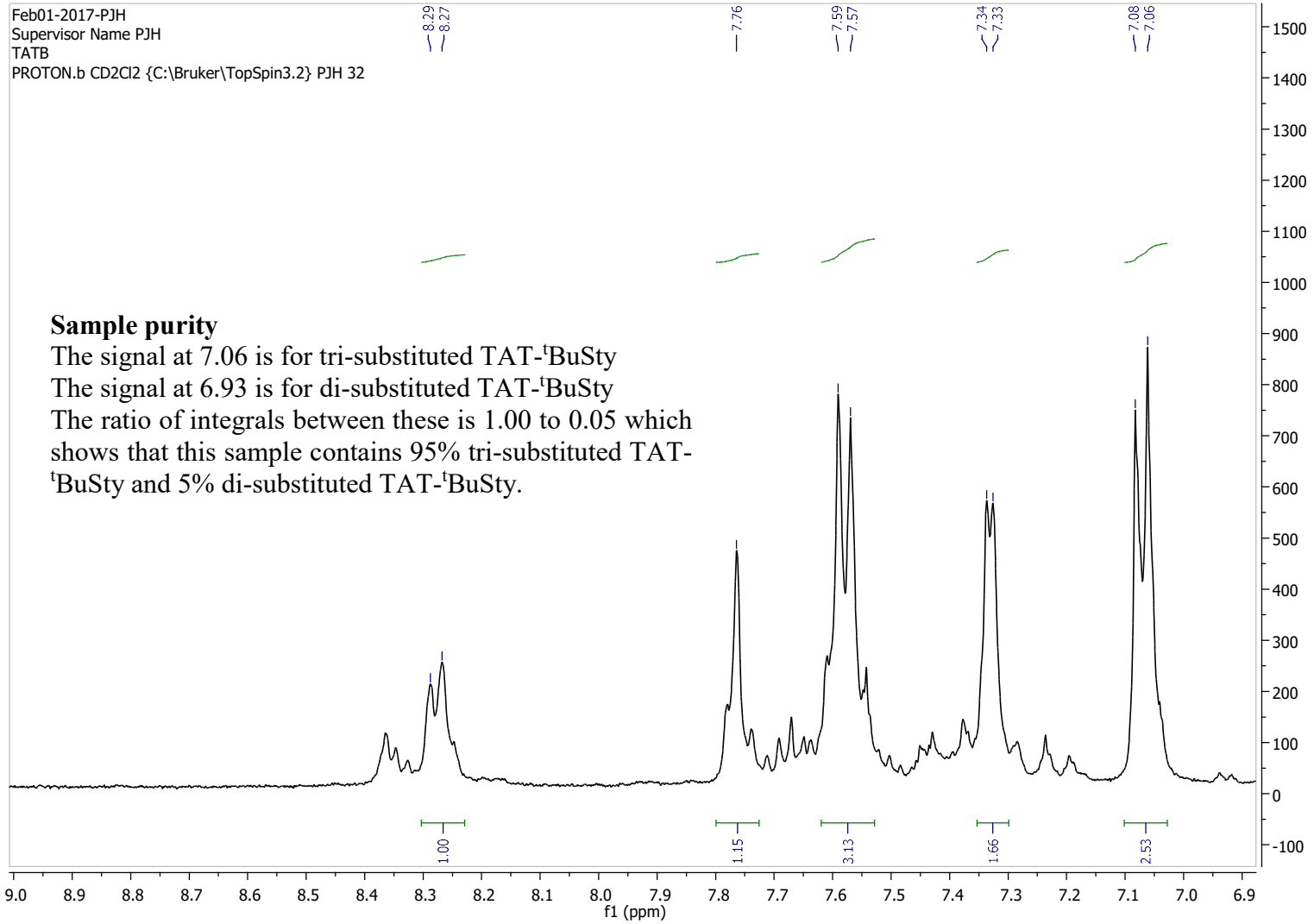

S2.3 Expansion of methylene and methyl resonance region of ^{1}H NMR spectrum of TAT-^{t}BuSty with peak picking and integration analysis

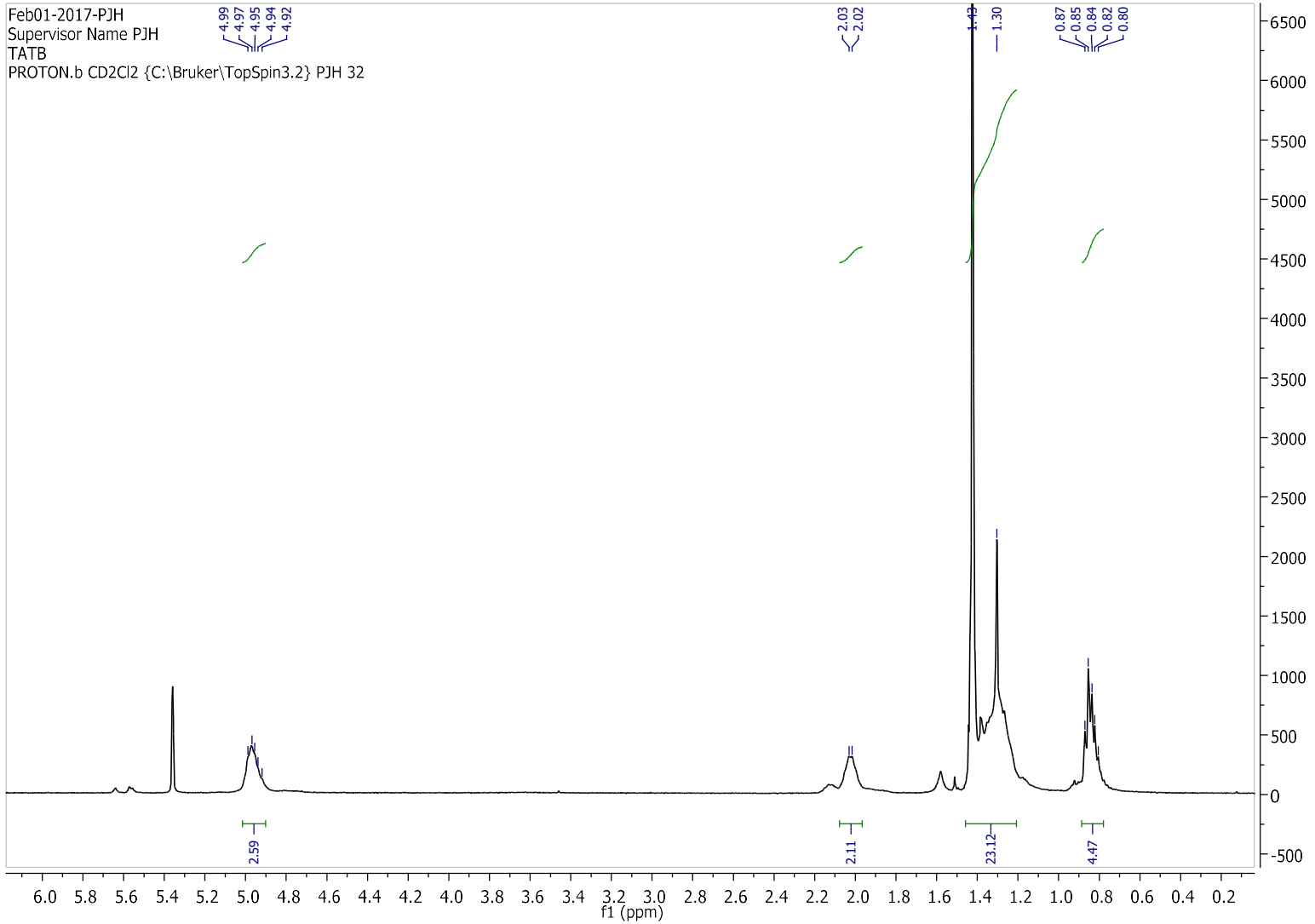

S2.4 ^{13}C NMR Spectrum for TAT-^{t}BuSty with peak picking

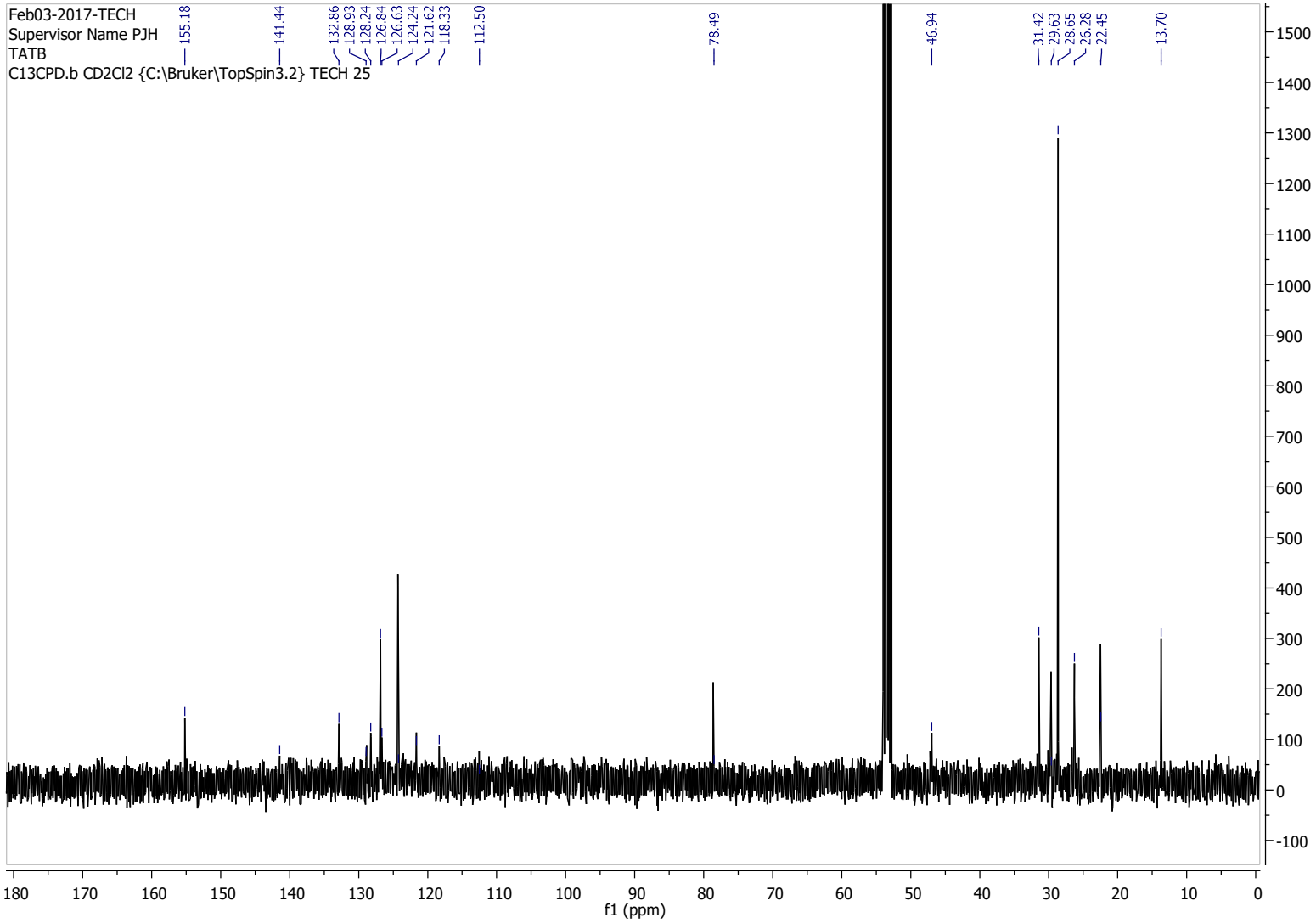

S2.5 Theoretical estimation of ^{13}C NMR Spectrum for TAT-^{t}BuSty

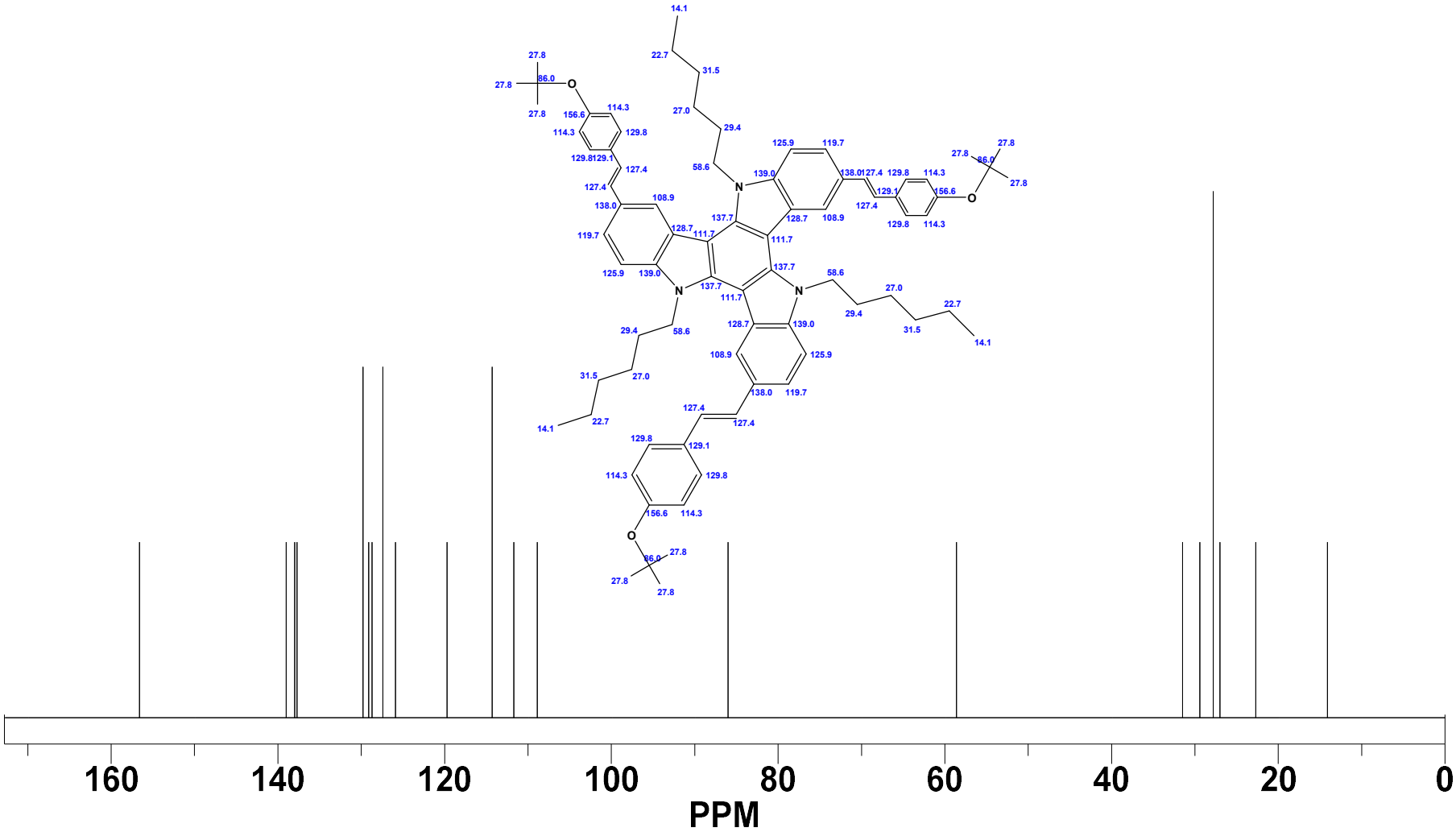

S3 High Resolution Mass Spectrometry of TAT-^{t}BuSty analysed using positive electrospray

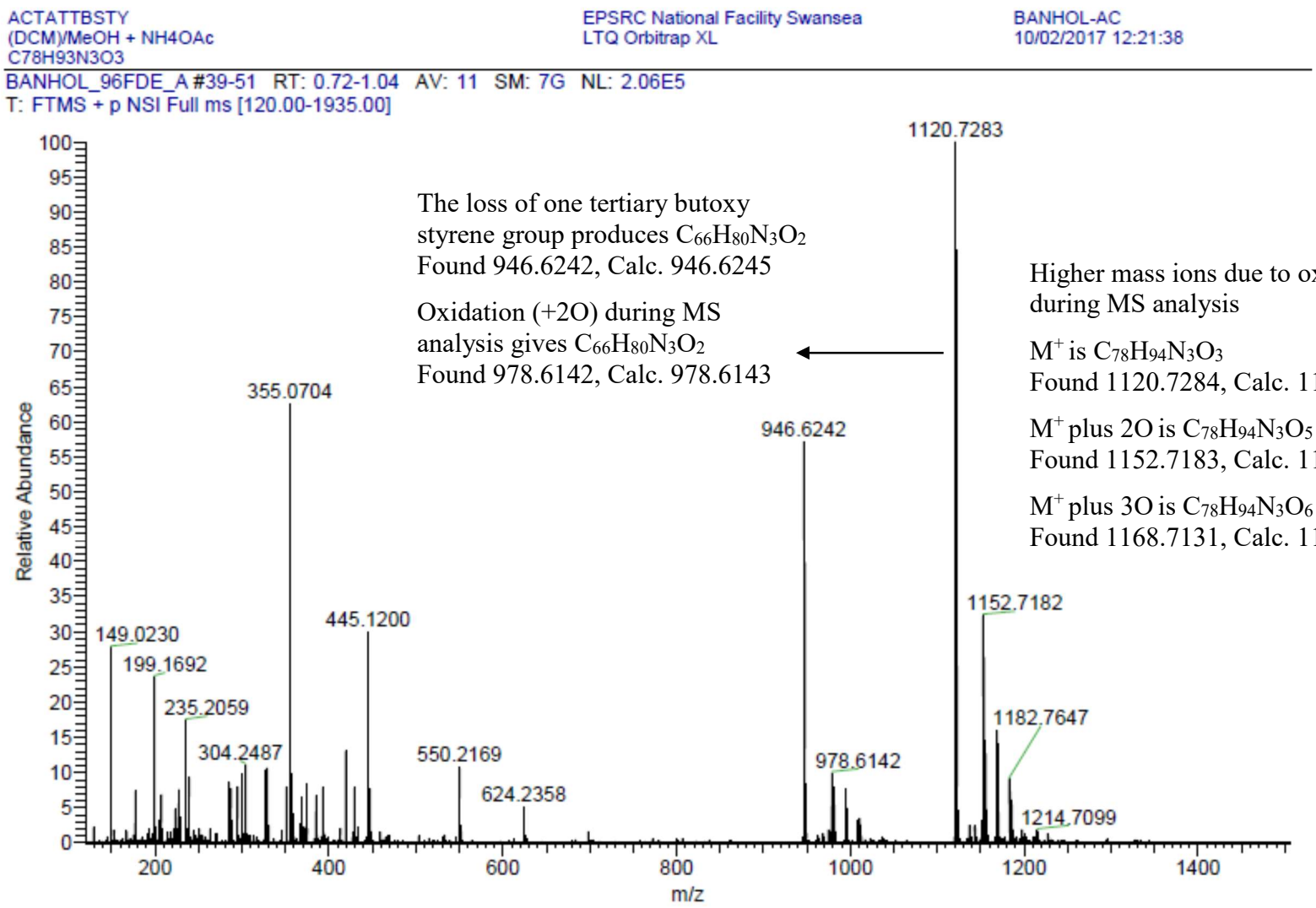

S3.1 Observed data & theoretical isotope pattern from positive electrospray high resolution mass spectrometry of TAT-^{t}BuSty

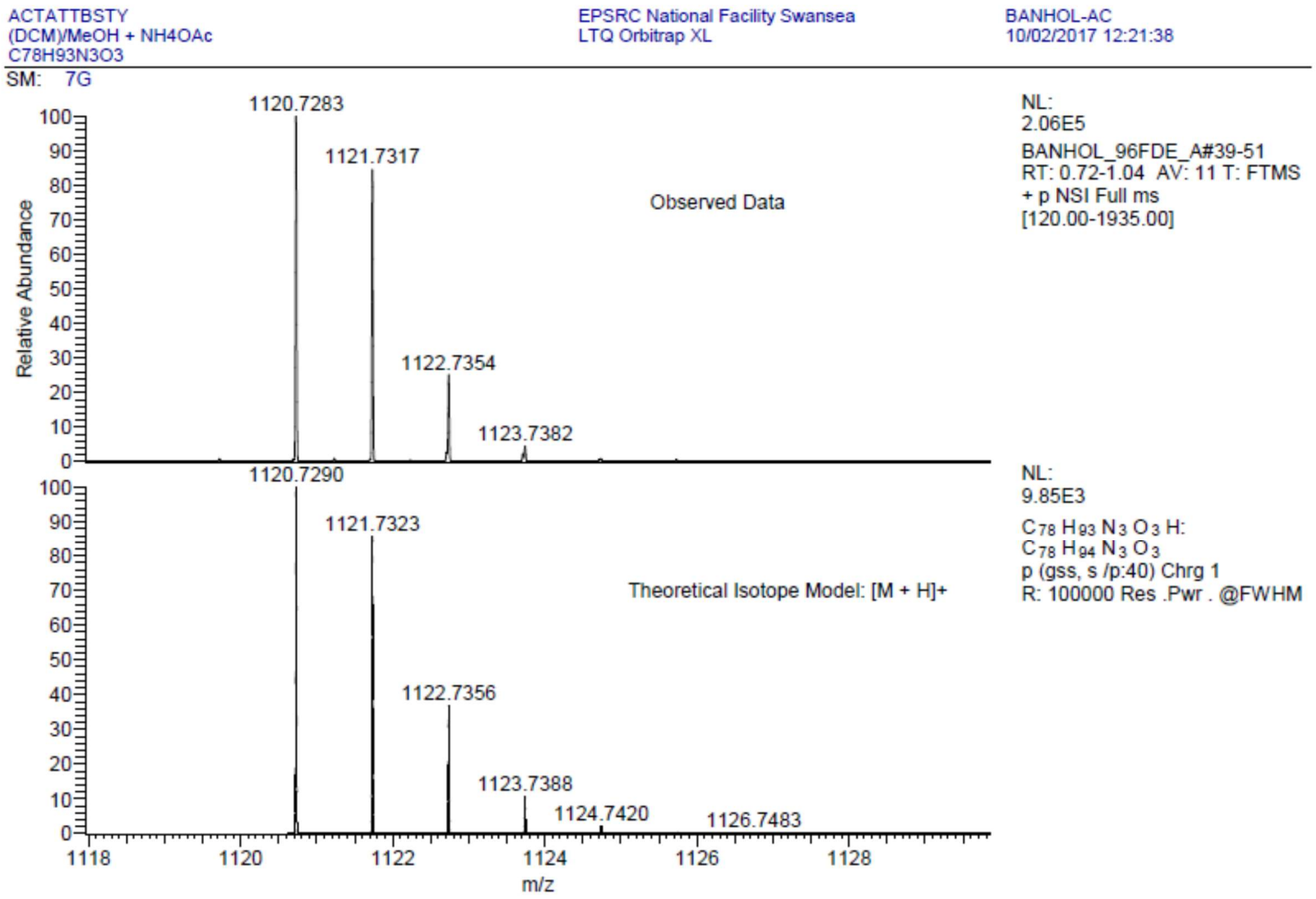

S4 - Route 1 Cost Analysis Table for TAT-^{t}BuSty

* = *trans*-di(m-acetato)bis[O-(di-o-tolylphosphino)benzyl]diPd(II)

Chemical	Reagent mass (g)	Solvent Vol. (ml)	Reagent cost ($/g)	Solvent cost ($/ml)	Reagent + solvent cost ($)	Product cost ($/g)
Oxindole	10		2.29		22.9	
$POCl_3$	150		0.13		19.7	
NaOH	250		0.013		3.3	
Anhydrous $MgSO_4$	10		0.066		0.7	
Silica	200		0.13		26.2	
Methanol		500		0.013	6.6	
CH_2Cl_2		5500		0.013	72.1	
Total	**620**	**6000**			**151.5**	
Product step 1 (Yield = 65%, 5.5g)						**27.5**
Sodium Hydride	0.2		2.18		0.43	
Anhydrous DMF		2		0.08	0.16	
Iodohexane	2		0.4		0.86	
Anhydrous $MgSO_4$	1		0.066		0.066	
Silica	20		0.13		2.62	
Petroleum-Ether		500		0.013	6.55	
Dichloromethane		100		0.013	1.31	
Total	**23.2**	**652**	**2.80**	**0.1**		
Product step 2 (Yield = 75%, 1.3g)						**9.2**
N-Bromosuccinimide	1		0.09		0.09	
Anhydrous $CHCl_3$		90		0.066	5.9	
Anhydrous DMF		15		0.08	0.12	
Anhydrous $MgSO_4$	1		0.066		0.066	
Silica	20		0.13		2.62	
Petroleum-Ether		500		0.013	6.55	
Dichloromethane		125		0.013	1.64	
Total	**22**	**730**			**17**	
Product step 3 (Yield = 82%, 1.35g)						**12.6**
Tertiary butoxystyrene	0.68		1.3		0.89	
Anhydrous $CH_3CON(CH_3)_2$		10		0.08	0.8	
Anhydrous Na_2CO_3	0.25		0.066		0.013	
Pd cat*	0.045		101		4.55	
Magnesium $MgSO_4$	0.5		0.066		0.04	
Silica	20		0.13		2.62	
Dichloromethane		125		0.013	1.64	
Petroleum ether		500		0.013	6.55	
Total	**21.48**	**635**			**17.1**	
Product step 4 (Yield = 95%, 0.83g)						**20.6**
Total solvent mass & vol.	**686.68**	**8017**				
Product Cost						**69.9**

S4.1 - Route 1 Cost Analysis Table for SP12

* [1,1′-bis(diphenylphosphino)ferrocene]dichloropalladium(II)

Chemical Name	Reagent mass (g)	Solvent Vol. (ml)	Reagent cost ($/g)	Solvent cost ($/ml)	Reagent + solvent cost ($)	Product cost ($/g)
Oxindole	10		2.29		22.9	
$POCl_3$	150		0.13		19.7	
NaOH	250		0.013		3.3	
Anhydrous $MgSO_4$	10		0.066		0.7	
Silica	200		0.13		26.2	
Methanol		500		0.013	6.6	
Dichloromethane		5500		0.013	72.1	
Total	**620**	**6000**			**151.5**	
Product step 1 (Yield = 65%, 5.5g)						**27.5**
Sodium Hydride	0.2		2.18		0.43	
Anhydrous DMF		2		0.08	0.16	
Iodoethane	2		0.4		0.86	
Anhydrous $MgSO_4$	1		0.066		0.066	
Silica	20		0.13		2.62	
Petroleum-Ether		500		0.013	6.55	
Dichloromethane		100		0.013	1.31	
Total	**23.2**	**652**	**2.80**	**0.1**		
Product step 2 (Yield = 75%, 1.3g)						**9.2**
N-Bromosuccinimide	1		0.09		0.09	
Anhydrous $CHCl_3$		90		0.066	5.9	
Anhydrous DMF		15		0.08	0.12	
Anhydrous $MgSO_4$	1		0.066		0.066	
Silica	20		0.13		2.62	
Petroleum ether		500		0.013	6.55	
CH_2Cl_2		125		0.013	1.64	
Total	**22**	**730**			**17**	
Product step 3 (Yield = 82%, 1.35g)						**12.6**
Paramethoxybenzene Boronic Acid	0.61		13.1		8	
Anhydrous Toluene		10		0.026	0.26	
Anhydrous Methanol		5		0.026	0.13	
Pd catalyst*	0.072		22.3		1.6	
Anhydrous $MgSO_4$	0.5		0.066		0.04	
Silica	20		0.13		2.62	
CH_2Cl_2		300		0.013	3.9	
Petroleum ether		900		0.013	11.8	
Total	**21.18**	**1215**			**28.35**	
Product step 4 (Yield = 86%, 0.64g)						**44.3**
Total mass & solvent volume	**686.382**	**8597**				
Product Cost						**93.6**

S4.2 - Synthesis of TAT-^{t}BuSty via route 2

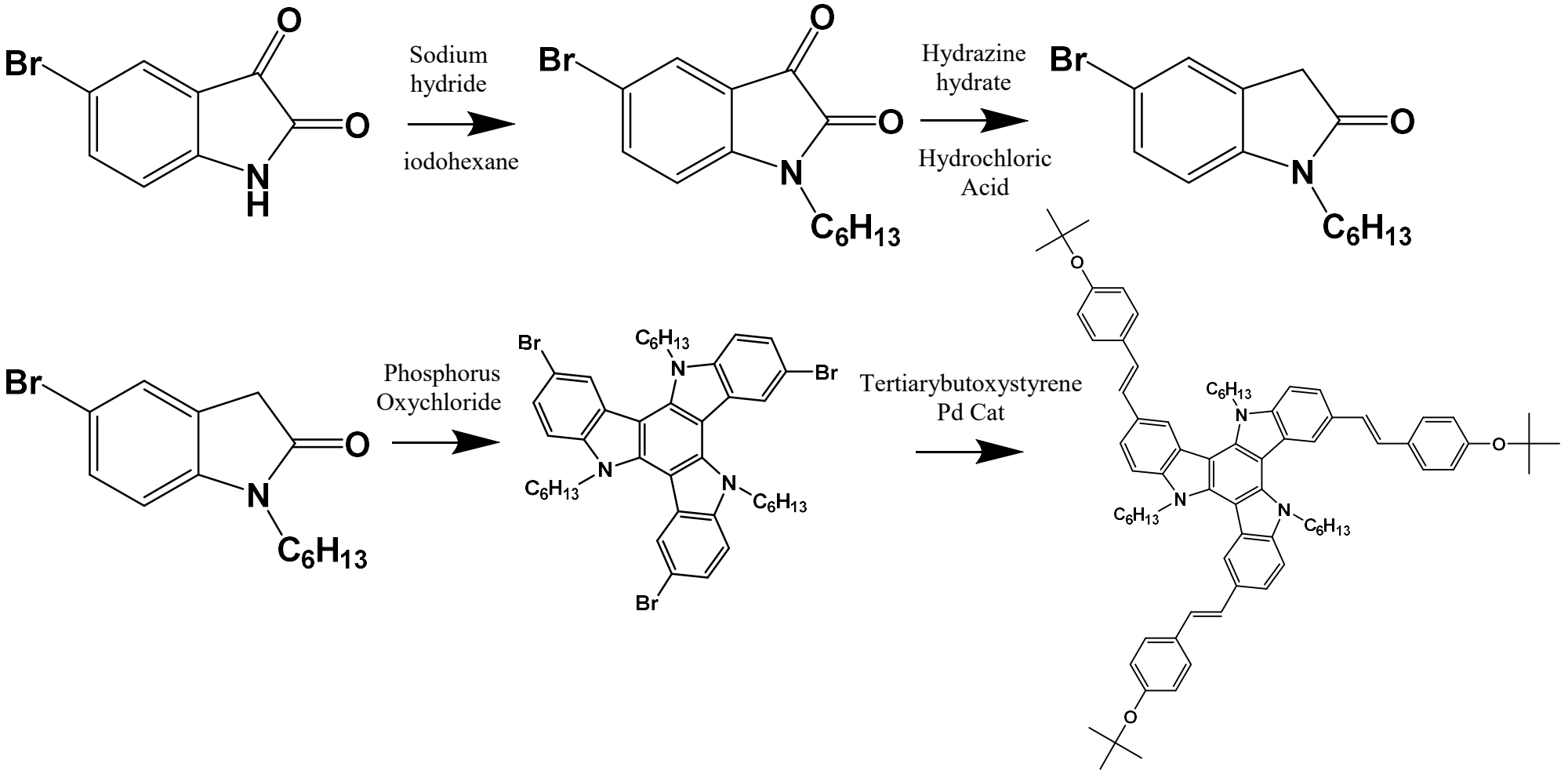

S4.3 Route 2 Cost Analysis Table for TAT-^{t}BuSty

* Trans-di(m-acetato)bis[O-(di-o-tolylphosphino)benzyl]dipalladium(II)

Chemical Name	Reagent mass (g)	Solvent Vol. (ml)	Reagent cost ($/g)	Solvent cost ($/ml)	Reagent + solvent cost ($)	Product cost ($/g)
5-Bromoisatin	10		0.77		7.7	
Sodium Hydride	1.06		2.17		2.31	
Anhydrous DMF		200		0.08	15.7	
Iodohexane	46.9		0.43		20.3	
Petroleum ether		250		0.013	3.3	
Total	**57.96**	**450**			**49.3**	
Product step 1 (Yield = 90%, 12.3g)						**4**
Hydrazine Hydrate	39		0.09		3.68	
$HCl_{(aq)}$	10		0.013	0.13	0.13	
Total	**49**				**3.81**	
Product step 2 (Yield = 64%. 2.73g)						**1.4**
$POCl_3$	50		0.13		6.55	
NaOH	250		0.013		3.28	
Anhydrous $MgSO_4$	10		0.066		0.66	
Silica	200		0.13		26.2	
Methanol		500		0.013	6.55	
CH_2Cl_2		5500		0.013	72.05	
Total	**510**	**6000**			**115.3**	
Product step 3 (Yield = 65%, 5.5g)						**21**
Tertiary butoxystyrene	0.68		1.3		0.9	
Anhydrous Dimethylacetamide		10		0.08	0.8	
Anhydrous Na_2CO_3	0.25		0.066		0.013	
Pd catalyst *	0.045		101		4.55	
Anhydrous $MgSO_4$	0.5		0.066		0.04	
Silica	20		0.13		2.62	
CH_2Cl_2		125		0.013	1.64	
Petroleum ether		500		0.013	6.55	
Total	**21.475**	**635**			**17.1**	
Product step 4 (Yield = 95%, 0.83g)						**20.6**
Total solvent mass & volume	**638.435**	**7085**				
Product Cost						**47**

S4.4 Summary of the donor group cost (Sigma Aldrich®) and coupling reaction yields for triazatruxene HTMs used to prepare perovskite devices with η > 18%

HTM	Donor group	Donor group molecular structure	Donor gp cost (£ g^{-1})	Yield (%)
TAT-^{t}BuSty[†]	Tert-butoxystyrene	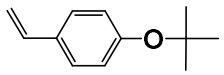	1	95
Trux-OMeTAD[ESI1]	Dimethoxy-diphenylamine	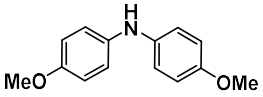	16	70
K131[ESI2]	Dimethoxy-diphenylamine	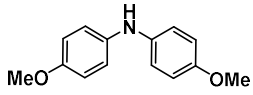	16	45
SP-12[ESI3]	4-methoxy-phenylboronic acid	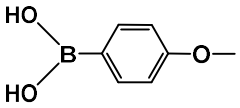	10	86

References

[†] This work

ESI1 Huang, C.; Fu, W.; Li, C-Z.; Zhang, Z.; Qiu, W.; Shi, M.; Heremans, P.; Jen, A. K-Y.; Chen, H. *J. Am. Chem. Soc.* **2016**, *138*, 2528−2531.

ESI2 Rakstys, K.; Abate, A.; Dar, M.I.; Gao, P.; Jankauskas, V.; Jacopin, G.; Kamarauskas, E.; Kazim, S.; Ahmad, S.; Grätzel, M.; Nazeeruddin, M.K. *J. Am. Chem. Soc.* **2015**, *137*, 16172−16178.

ESI3 Su, P-Y.; Huang, L-B.; Liu, J-M.; Chen, Y-F.; Xiao, L-M.; Kuang, D-B.; Mayor, M.; Su, C.-Y. *J. Mater. Chem. A.* **2017**, *5*, 1913-1918.

S5 Differential Scanning Calorimetry for the first (a) and second (b) heating cycles of TAT-^{t}BuSty (solid line) and spiro-OMeTAD (dashed line).
Heating at 10°C under N_2. Endothermic peaks are up

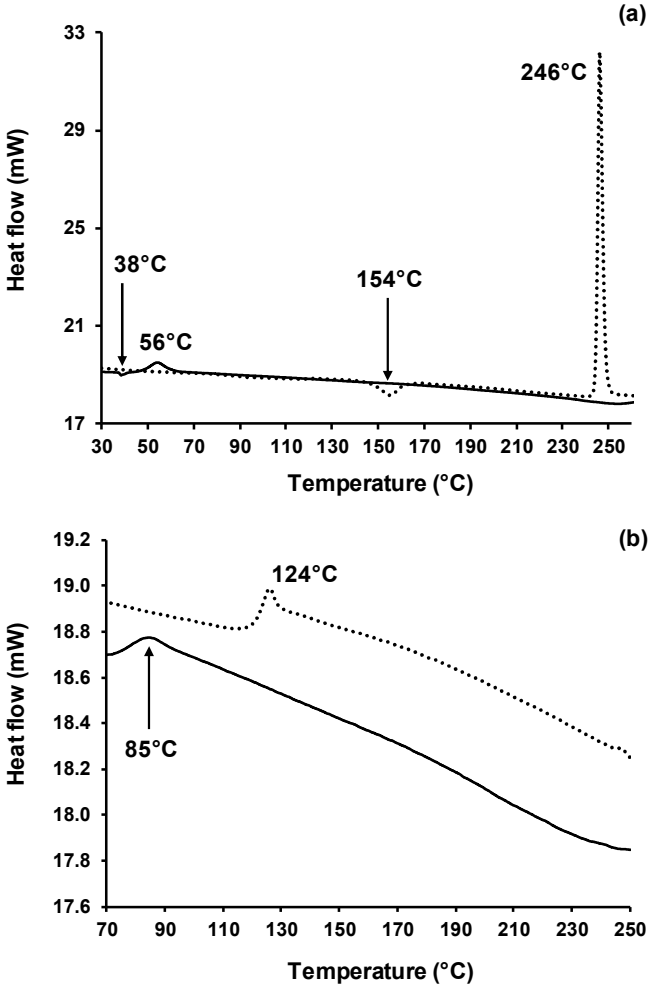

S6 - Contact angle measurements of water on (a) TAT-^{t}BuSty and (b) spiro-OMeTAD thin films

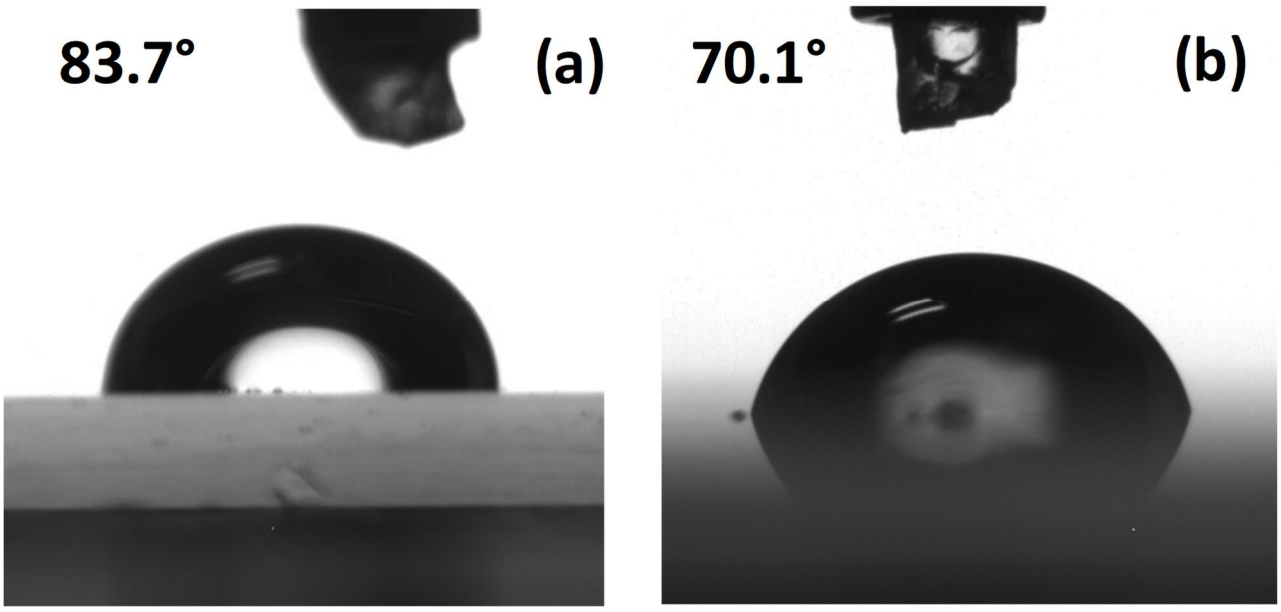

S7.1 - External calibration of electrochemistry using ferrocene (a) CV and (b) square wave voltammetry

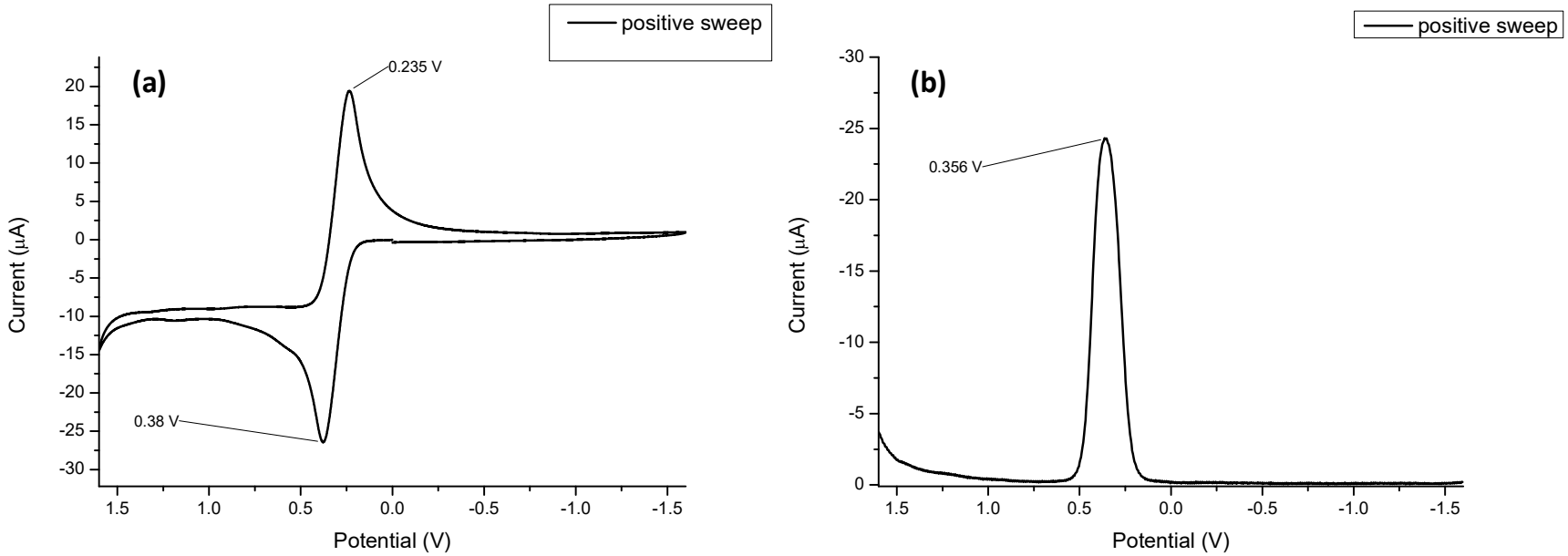

S7.2 - Electrochemistry of (3) showing (a) CV and (b) square wave voltammetry and of (5) showing (c) CV and (d) square wave voltammetry

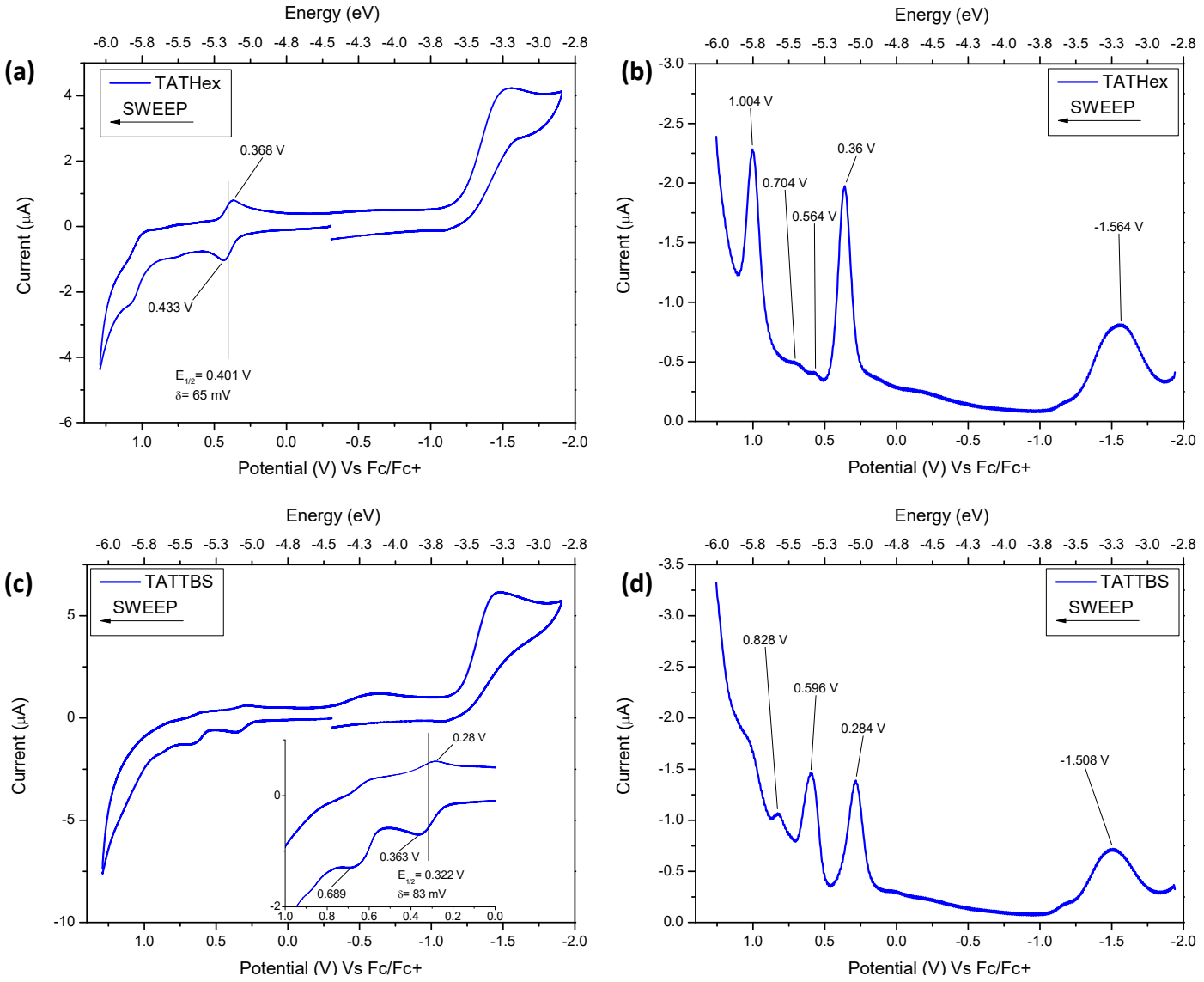

S7.3 Cyclic and square wave voltammograms of 3 and 5 (0.1mM) in dry DCM with NBu_4PF_6 (0.1M) as supporting electrolyte. Positive sweep at 0.1V.s^{-1}

Sample	CV		SWV	
	IP (V)	EA (V)	IP (V)	EA (V)
(3)	0.401 ∂: 65 mV (–5.2 eV)	irreversible	0.360 V (–5.2 eV)	–1.564 V (–3.2 eV)
(5)	0.322 ∂: 83 mV (–5.1 eV)	irreversible	0.284 V (–5.1 eV)	–1.508 V (–3.3 eV)

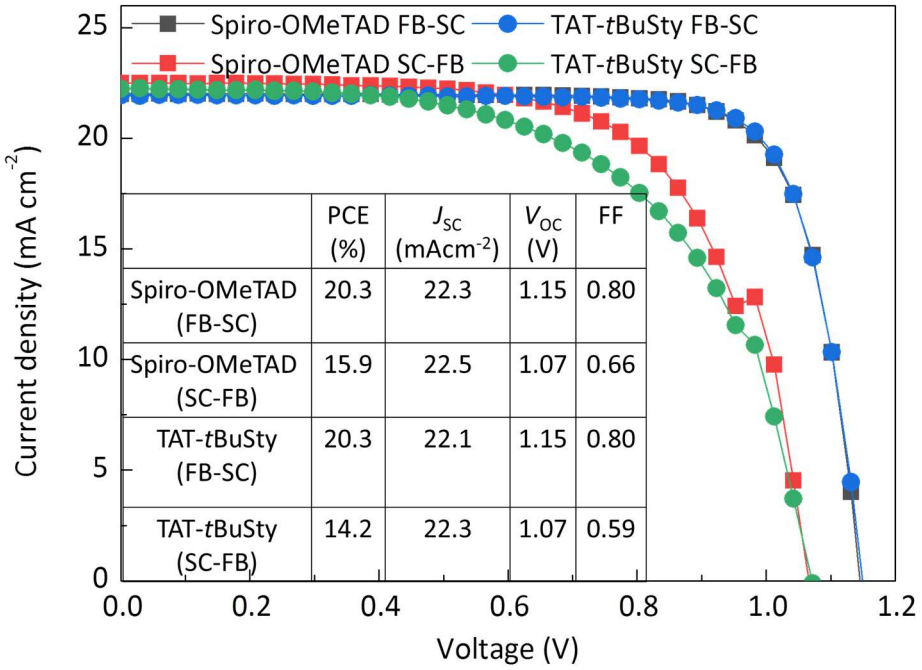

S8.1 Device performance using Spiro-OMeTAD and TAT-*t*BuSty as HTM layers. *J–V* characteristics of optimized perovskite solar cells with FTO/SnO_2/perovskite/HTM/Au device structure, scanned from forward bias (FB) to short circuit (SC) and back again at a scan rate of 0.38 V s^{-1}. Corresponding device characteristics are given in the embedded table.

S8.2 A comparison of the current-voltage parameters for TAT-^{t}BuSty with the next best performing truxene and triazatruxenes reported to date. Data for spiro-OMeTAD reported in side by side studies are also included.

HTM	Scan	η (%)	V_{oc} (V)	J_{sc} (mA cm^{-2})	FF
TAT-^{t}BuSty†	R	20.3	1.15	22.1	0.80
	F	15.7	1.07	22.2	0.66
Trux-OMETAD[ESI1]	R	18.6	1.02	23.2	0.79
	F	17.5	1.02	23.4	0.74
Spiro-OMETAD	R	16.3	0.99	23.0	0.72
KR131[ESI2]	R	18.3	1.15	20.7	0.77
	F	17.0	1.15	20.6	0.72
Spiro-OMETAD	R	17.9	1.09	22.3	0.74
	F	16.3	1.06	22.3	0.69
SP-12[ESI3]	R	18.8	1.08	22.8	0.77
	F	16.7	1.04	22.8	0.70
Spiro-OMETAD	R	16.9	1.02	21.6	0.77
	F	15.0	0.98	21.5	0.71
HPDI[ESI4]	R	10.8	0.98	19.2	0.58
Spiro-OMETAD	R	12.9	0.94	19.6	0.69
TBDI[ESI5]	R	14.9	1.09	18.7	0.73
	F	14.9	1.09	18.7	0.73
PEDOT:PSS/polyTPD*	-	15.3	1.08	18.5	0.76

† = this work, * Poly(N,N'-bis-4-butylphenyl-N,N'-bisphenyl)benzidine, R and F stand for reverse scan and forward scan, respectively.

ESI4. Ramos, F.J.; Rakstys, K.; Kazim, S.; Grätzel, M.; Nazeeruddin, M.K.; Ahmad, S. *RSC Adv.* **2015**, *5*, 53426-53432.
ESI5. Calió, L.; Momblona, C.; Gil-Escrig, L.; Kazim, S.; Sessolo, M.; Sastre-Santos, Á.; Bolink, H. J.; Ahmad, S. *Solar Energy Mater. Solar Cells.* **2017**, *163*, 237–241.

S9 X-ray diffraction data for films of (a) spiro-OMeTAD and (b) TAT-^{t}BuSty on FTO glass from Solaronix. The plain FTO substrate is shown in (c). These data confirm that no crystalline peaks are observed for either of these HTM films on FTO

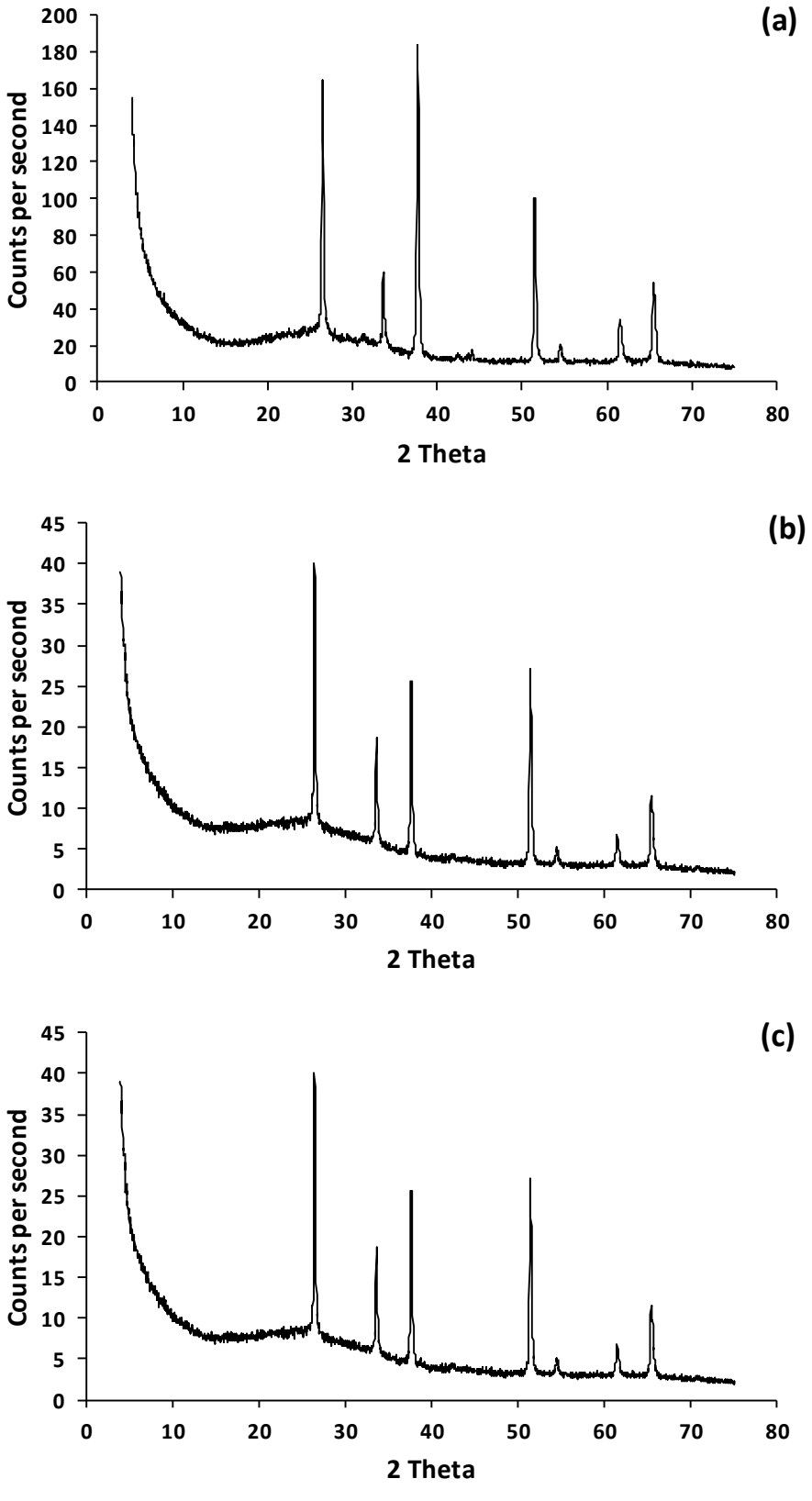

S10 HTM abbreviations

From Nazeeruddin *et al.*, *J. Am. Chem. Soc.* 2015, *137*, 16172−16178.
(K122) 5,10,15-trihexyl-3,8,13-trimethoxy-10,15-dihydro-5H-diindolo[3,2-a:3′,2′-c]carbazole
(K131) 5,10,15-trihexyl-3,8,13-tris(4-methoxyphenyl)-10,15-dihydro-5H-diindolo[3,2-a:3′,2′-c]-carbazole
(K133) 4,4′,4″-(5,10,15-trihexyl-10,15-dihydro-5Hdiindolo[3,2-a:3′,2′-c]carbazole-3,8,13-triyl)tris(N,N-bis(4-methoxyphenyl)aniline)
(K145) 5,10,15-trihexyl-N^3,N^3,N^8,N^8,N^{13},N^{13}-hexakis(4-methoxyphenyl)-10,15-dihydro-5H-diindolo[3,2-a:3′,2′-c]carbazole-3,8,13-triamine

From Chen *et al.*, H. *J. Am. Chem. Soc.* 2016, *138*, 2528−2531.
(TruxOMeTAD) 3,8,13-tri(di-4-methoxylphenylamino)-5,5,10,10,15,15-Hex(1-hexyl)10,15-dihydro-5H-diindeno[1,2-α;1’,2’-c]fluorene

From Su et al., *J. Mater. Chem. A.* 2017, *5*, 1913-1918.
(SP11) 2,7,12-tris(*N,N*-bis(4-methoxyphenyl)aniline)-5,10,15-triethyltriindole
(SP12) 2,7,12-tris(4-methoxyphenyl)-5,10,15-triethyltriindole

From Nazeeruddin et al., *RSC Adv.* 2015, *5*, 53426-53432.
(HPDI) 5,10,15-Tris(4-(hexyloxy)phenyl)-10,15-dihydro-5H-diindolo[3,2-a:3’,2’-c]carbazole

S11a Digital images of TAT-^{t}BuSty HTM films either cycled through 30 min at 80°C followed by 30 min in air or exposed to ambient air

S11b Analysis of the red, green and blue (RGB) components of the digital images of the spiro-OMeTAD (dashed lines) and TAT-^{t}BuSty (solid lines) across the heating cycles of 30 min at 80°C followed by 30 min in ambient air

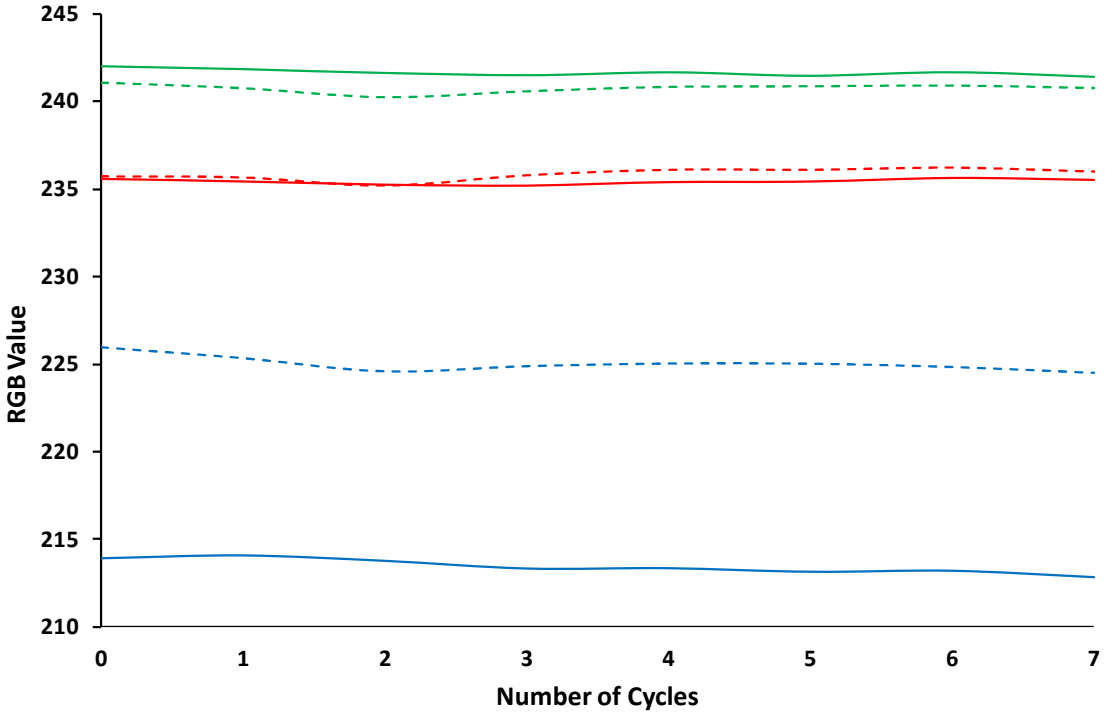

S11c UV-visible spectra of (a) spiro-OMeTAD control - ambient air and temperature, (b) heat cycled spiro-OMeTAD, (c) TAT-^{t}BuSty control - ambient air and temperature and (d) heat cycled TAT-^{t}BuSty. Heat cycles were 30 min at 80°C followed by 30 min in ambient air